



Performance of various predicted GNSS global ionospheric maps relative to GPS and JASON TEC data

Min Li^{1,3} · Yunbin Yuan¹ · Ningbo Wang² · Zishen Li² · Xingliang Huo¹

Received: 29 August 2017 / Accepted: 21 March 2018 / Published online: 27 March 2018
© Springer-Verlag GmbH Germany, part of Springer Nature 2018

Abstract

When using predicted total electron content (TEC) products to generate preliminary real-time global ionospheric maps (GIMs), validation of these ionospheric predicted products is essential. In this study, we evaluate the accuracy of five predicted GIMs, provided by the international GNSS service (IGS), over continental and oceanic regions during the period from September 2009 to September 2015. Over continental regions, the GPS TEC data collected from 41 IGS continuous tracking stations are used as a reference data set. Over oceanic regions, the TEC data from the JASON altimeter are used for comparison. An initial performance comparison between the IGS combined final GIM product and the predicted GIMs is also included in this study. The evaluation results show that the predicted GIMs produced by CODE outperform the other predicted GIMs for all three validation results. The accuracy of the 1-day predicted GIMs, produced by the IGS associate analysis centers (IAACs), is higher than that of the 2-day predicted GIMs. Compared to the 2-day UPC predicted GIMs, the 2-day ESA predicted GIMs are observed to have slightly worse performances over ocean regions and better positioning performances over continental regions.

Keywords GNSS · Total electron content (TEC) · Predicted global ionospheric maps (GIMs) · JASON altimeter

Introduction

Single-frequency (SF) global navigation satellite system (GNSS) users need additional corrections to remove signal degradation caused by the ionosphere since the ionospheric delay errors can be as much as tens of meters in the zenith direction (Komjathy and Langley 1996; Leick et al. 2015). The existence of the worldwide international GNSS service (IGS) permanent network of dual-frequency receivers makes the computation of global ionospheric maps (GIMs) of total electron content (TEC) feasible (Yuan et al. 2015). Currently, the IGS associate analysis centers (IAACs) generate

three types of ionospheric products—final, rapid and predicted GIMs—using the ionosphere map exchange format (Hernández-Pajares et al. 2017). The final and rapid GIMs are systematically produced on a daily basis with latencies of 1–2 weeks and 1 day, respectively (Hernández-Pajares et al. 2009). A number of studies evaluating the accuracy of the final GIMs have shown that the final GIMs are able to provide not only highly accurate but also highly reliable ionospheric TEC data (Feltens 2003).

Ionospheric predictions are of considerable importance for certain scientific and technological applications (Krankowski et al. 2005). Specifically, ionospheric predictions can be used as background models to generate preliminary real-time GIMs (García-Rigo et al. 2011). Predicting the conditions in the earth's ionosphere is among the major tasks of the fields of solar-terrestrial physics and space weather (Cander 2003; Zolesi and Cander 2014).

At present, there are three IAACs that together generate five types of predicted ionospheric products: the 1- and 2-day vertical TEC (VTEC) maps produced by CODE (Center for Orbit Determination in Europe, University of Berne, Switzerland) (named C1PG and C2PG), the 1- and 2-day VTEC maps produced by ESA/ESOC (European Space Operations

✉ Min Li
limin@asch.whigg.ac.cn

✉ Yunbin Yuan
yybgps@whigg.ac.cn

¹ State Key Laboratory of Geodesy and Earth's Dynamics, Institute of Geodesy and Geophysics, Wuhan, China

² Academy of Opto-Electronics, Chinese Academy of Sciences, Beijing, China

³ University of Chinese Academy of Sciences, Beijing, China

Center of ESA, Darmstadt, Germany) (named E1PG and E2PG), and the 2-day VTEC maps produced by UPC (Technical University of Catalonia, Barcelona, Spain) (named U2PG). These predicted GIMs provided by the IAACs have been available to the public since September 2009 via the Crustal Dynamics Data Information System (CDDIS; <ftp://cddis.gsfc.nasa.gov/gps/products/ionex/>). According to previous studies, these predicted products are computed by either extrapolation methods or models that are based on a physical concept. For example, the CODE predicted product is based on the extrapolation of spherical harmonic coefficients (Schaer 1999), and the UPC ionospheric VTEC prediction model is based on linear regression and the discrete cosine transform (García-Rigo et al. 2011).

It has been recognized that real-time ionospheric models are required for near real-time products based upon current ionospheric specifications (Gulyaeva et al. 2013). However, no real-time GIM is available from the IAACs at present. Fortunately, if the predicted IGS GIMs are validated to have high precision, they can be used to provide TEC corrections for mass market SF receivers, instead of real-time ionospheric models, in applications such as automobiles, personal navigation and logistics. Since the predicted GIMs from the different IAACs are computed based on different processing strategies, their accuracy performances tend to be different. Thus, it is necessary to assess the performance of the predicted GIMs from different IAACs in terms of correcting the ionospheric delay. However, limited knowledge is available regarding the performance validation of predicted GIMs. Although García-Rigo et al. (2011) compared the accuracy of the CODE, ESA and UPC 2-day predicted products against JASON data, their studies were based on the period of day of year (DOY) 184–355, 2010. Analysis of long periods of predicted GIMs from different IAACs based on multiple evaluation methods has not yet been systematically studied. Thus, the main goal of this research is to present a comparison and analysis of the accuracy of a long time series of predicted GIMs from the three IAACs (CODE, UPC, and ESA). We believe that our analysis results can provide SF GNSS users with some practical suggestions or valuable references on how to choose a suitable ionospheric predicted product to satisfy the need to estimate real-time ionospheric GIMs for real-time positioning.

Extensive studies have already been carried out regarding the performance of GIMs (Orus et al. 2002). The representative assessment methods can generally be classified into three categories: (1) comparison between the VTEC predictions in GIMs with TOPEX or JASON data, which provide an independent and precise TEC determination over the oceans (Brunini et al. 2005); (2) comparison between the VTEC predictions in GIMs with the measured ionospheric TEC using GNSS data (Wang et al. 2017); and (3) validation against the IGS combined final products (designated

IGSG). In this study, three schemes based on the method listed above are adopted for a comprehensive accuracy assessment of predicted GIMs. GNSS TEC data generated from 41 IGS GNSS receivers worldwide and TEC data from the JASON altimeter are used for comparison. In addition, the IGS combined final product is also used as a reference to validate the performance of the predicted GIMs.

Data sets and methodology

In order to present a statistically representative result, we examined the accuracy of all accessible predicted IGS GIMs based on the methods mentioned above over a time period of 6 years, from the initiation of predicted IGS ionospheric production on September 1, 2009, to September 30, 2015. The selected period includes conditions of both low and high solar and geomagnetic activity. According to the studies of Wang et al. (2016) and Hoque et al. (2017), the GPS broadcast model in the navigation message can mitigate the ionospheric delay range from 49.5 to 55%. Therefore, the predicted GIM was regarded as invalid in this study when its accuracy was lower than that of the GPS broadcast model. Additionally, the predicted GIM was marked as unavailable in the case it cannot be downloaded from the main IGS server. Also note that days on which any one of the predicted IGS products was marked as invalid or unavailable were discarded in the assessment. An invalid ionospheric grid point whose TEC value is set to 999.9 TECU is not used in the performance assessment. The daily statistics for a specific predicted GIM file is computed based on the valid ionospheric grid points only.

Note that the sampling time of the IGS GIMs is 1 or 2 h, whereas the VTEC values derived from the JASON data and GNSS observations are presented as a function of time, latitude and longitude. Therefore, when the IGS GIMs are compared with the altimeter and GNSS measurements, the GIM TEC predictions should be interpolated to the same GNSS or JASON footprint locations and times by adopting a bivariate spatial interpolation scheme in a solar-fixed reference frame and a linear time interpolation between two consecutive GIMs (Schaer 1999). The VTEC differences thus obtained are used to compute different kinds of statistics, including mean daily offsets and related root mean square (RMS) values, for each IAAC product.

Validation against JASON TEC

The onboard radar altimeter of the JASON satellite, operating at a mean orbital height of approximately 1330 km (Orus et al. 2007), has dual-band emission with a Ku-band main frequency and a C-band auxiliary frequency (Lambin et al. 2010). Thus, JASON TEC can be derived from the dual-frequency radar altimeter signals along the ray path from the

satellite to the sea surface (Azpilicueta and Brunini 2009). As shown in Fig. 1, the ground tracks of JASON observations cover most of the global ocean between the latitudes 66°N and 66°S within 1 day. Therefore, as an independent and reliable source of VTEC, the JASON TEC data can be used as a reference to validate the performance of the predicted IGS GIMs over the ocean (except in polar regions) where there are few GNSS stations.

Note that the JASON TEC measurements have a systematic bias of approximately 2–5 TECU (10^{16} electrons/m²) above the real ionospheric TEC values (Jee et al. 2010). Additionally, the missing plasmaspheric electron content (PEC) in the computation of JASON TEC can be neglected at high latitudes but can reach 8 TECU at the equator (Orus et al. 2002; Lee et al. 2013). Even so, the JASON observations are still known to be one of the most accurate TEC data sets currently available and have been used to validate IGS GIMs in difficult conditions, over the ocean, and typically far from receivers (Hernández-Pajares et al. 2009, 2017). Therefore, JASON TEC measurements are used to assess errors in the different predicted GIMs in this study.

Validation against GPS TEC

In order to evaluate the quality of different predicted GIMs over continents, the GNSS dual-frequency derived ionospheric TEC values are compared to the corresponding TEC values interpolated from the predicted IGS GIMs on a point-by-point basis.

In general, the validation of predicted IGS GIMs against GPS TEC comprises four main steps. First, extract ionospheric observables, i.e., the sum of line-of-sight TEC and satellite-plus-receiver differential code biases (DCBs), from geometry-free linear combinations of undifferenced GNSS pseudorange and carrier phase measurements at each monitoring station (Brunini and Azpilicueta 2009). Because

pseudoranges leveled by carrier phases are free of ambiguities and have lower noise and fewer multi-path effects than pseudoranges (Li et al. 2017), we use the carrier-to-code leveling process for an individual satellite in consecutive arcs to obtain ionospheric information (Mannucci et al. 1998).

Second, we determine the actual slant TEC (STEC) by separating the satellite- and receiver-specific DCBs from the original ionospheric observables, which reads,

$$A \cdot \text{STEC}_i^k = \tilde{P}_{i,GF}^k - c \cdot B^k - c \cdot B_i + \varepsilon \tag{1}$$

where STEC_i^k is the line-of-sight ionospheric TEC along the signal propagation path from a GPS satellite k to a receiver i , ignoring higher-order contributions; $A = 40.31 \times 10^{16} \times (f_1^{-2} - f_2^{-2})$ (m/TECU); f_1 and f_2 are the frequencies of the GNSS satellite carrier phase observations; $\tilde{P}_{i,GF}^k$ represents the geometry-free combination of carrier phase ionospheric observable “leveled” to the code-delay ionospheric observable; B^k and B_i denote the satellite- and receiver-specific DCBs, respectively; c is the speed of light; and ε represents the unmodeled errors, such as observational noise and multi-path effects (Komjathy et al. 2005).

Third, the STEC is converted into VTEC using the mapping function

$$\begin{cases} \text{STEC} = \text{VTEC} \cdot \text{MF}(z) \\ \text{MF}(z) = [1 - \sin^2 z \cdot R_E^2 / (R_E + H_{\text{ion}})^2]^{-1/2} \end{cases} \tag{2}$$

under the single layer model (SLM) assumption (Wielgosz et al. 2003), where MF is the mapping function; z is the satellite zenith distances at the observation point; H_{ion} is the altitude of the ionospheric thin-layer shell, which is set to 450 km in this study; and R_E represents the mean radius of the earth (Yuan et al. 2008).

Fourth, compare the GPS TEC and the GIMs-interpolated TEC. In this study, the satellite and receiver DCBs are obtained from the monthly DCB products provided by CODE (Keshin 2012).

The precision of the GPS TEC obtained from the leveled carrier phase ionospheric observable is affected by significant intraday variations in receiver DCBs and leveling errors, produced by code delay noise and multi-path effects through the leveling procedure. Ciralo et al. (2007) found that leveling errors vary from ± 1.4 to ± 5.3 TECU and that intraday variation in receiver code delay DCB range from ± 1.4 to ± 8.8 TECU. The study of Brunini and Azpilicueta (2010) showed that during periods of high solar activity, the accuracy of the estimated STEC reaches approximately of ± 10 TECU for low geomagnetic regions and that during periods of low solar activity, the accuracy can be assumed to be on the order of ± 2 TECU.

Considering most GNSS users are operating low-cost, SF receivers, the performance of the predicted TEC on SF precise positioning accuracy (PPP) is also analyzed using

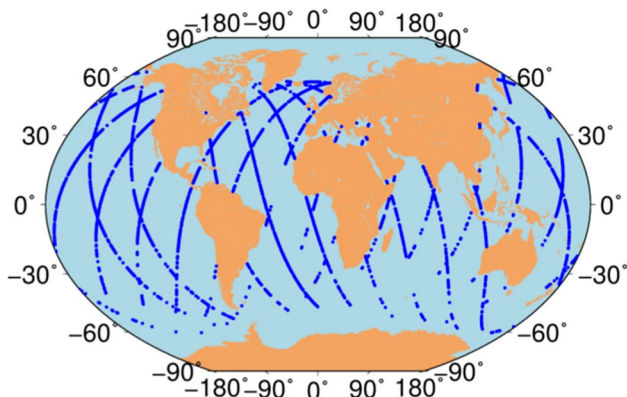


Fig. 1 Ground tracks of JASON satellites on June 13, 2013

post processing data from selected static IGS stations. When implementing SF PPP, the receiver positions were calculated using only the observations on the L1 frequency and the satellite elevation mask angle set to 7°. The zenith tropospheric delays were estimated as piece-wise constants with an update rate of 2 h. The IGS final products were used to determine the satellite position and clock offset. The zenith-referenced standard deviation is set as 60 cm for the code and 0.3 cm for the phase. The monthly satellite P1P2 DCB products provided by CODE are applied in the SF PPP processing. Corrections for solid earth tides, ocean tide loading and sub daily pole and nutation motions were also considered. The estimated coordinates based on ionospheric correction computed from different predicted GIMs are compared with the external coordinates obtained through the IGS weekly combination.

The locations of the selected 41 IGS stations over continental regions are shown in Fig. 2. The stations are distributed evenly across the globe and can represent well the ionospheric conditions at high, middle and low latitudes.

Validation against the IGS combined final GIM product

The IGS combined final TEC maps, which are computed as the weighted mean of the individual GIMs produced by different IAACs, have been generated without interruption since 1998 (Feltens et al. 2011). Previous work has validated that the IGS combined final GIM product has an estimated accuracy of 2–8 TECU and is slightly better than any of the individual IAAC maps (see <http://www.igs.org/products>). Therefore, the IGS combined final GIM product, which has been acknowledged as the most accurate post-processed TEC products, have been used as a reference in the performance assessment of the predicted GIMs.

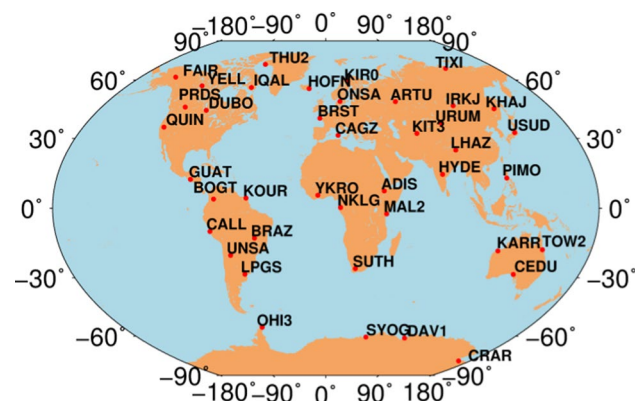


Fig. 2 Map showing the distribution of selected IGS receivers

Statistical indices

Five statistical indices are used to quantify the performance of the predicted GIMs provided by the different IAACs: the bias, standard deviation (STD), RMS of the differences between interpolated VTEC values from IGS GIMs and the reference TEC values, the relative STD ($STD_{relative}$) and RMS ($RMS_{relative}$) error with respect to the reference TEC values (Luo et al. 2013). The equations are as follows:

$$\begin{aligned} \text{Bias} &= \langle TEC_g - TEC_o \rangle \\ \text{Std} &= \sqrt{\langle (TEC_g - TEC_o - \text{bias})^2 \rangle} \\ \text{Rms} &= \sqrt{\langle (TEC_g - TEC_o)^2 \rangle} \end{aligned} \quad (3)$$

$$\text{Std}_{relative} = \text{std} / \langle TEC_o \rangle$$

$$\text{Rms}_{relative} = \text{rms} / \langle TEC_o \rangle$$

where TEC_g is the TEC obtained from predicted GIMs; TEC_o is the reference TEC derived from GPS, JASON satellites, or the combined final GIMs; and the symbol $\langle \cdot \rangle$ is the expectation operator for the given time span.

Results and discussion

The predicted IGS GIMs from different IAACs (the comparison data) are compared to the TEC observations provided by the JASON altimeter and the measured ionospheric TEC collected by the receivers shown in Fig. 2 for the test period. For comparison, the validation results of the IGS combined final GIMs against JASON and GPS TEC observations are included as a reference. In addition, as a third validation of the results, the consistency between predicted GIMs and the IGS combined final GIM products are also validated.

Validation against JASON TEC

Table 1 shows the bias, STD, RMS, mean VTEC, relative STD and relative RMS of the differences between IGS GIMs and JASON TEC for the test period. Note that since the TEC value of 999.9 TECU is defined as unavailable in the GIM file, there are slight differences between the numbers of JASON observations used for different predicted GIMs validation. Compared to the predicted GIMs, more observations have been used in the performance assessment of the IGS combined final GIM product.

As summarized in Table 1, the IGS combined final GIM product shows the best match with JASON TEC data, and

Table 1 Statistics of the differences between final and predicted IGS GIMs (IGSG, C1PG, C2PG, E1PG, E2PG and U2PG) and the JASON reference data, including bias, STD, RMS, mean VTEC, relative STD and RMS for the test period

	BIAS (TECU)	STD (TECU)	RMS (TECU)	VTEC (TECU)	STD/VTEC (%)	RMS/VTEC (%)	Number of observations
IGSG	1.42	4.07	4.31	21.77	18.68	19.78	3,130,177
C1PG	0.39	5.55	5.56	21.36	25.97	26.03	2,330,377
C2PG	0.49	5.65	5.67	21.36	26.45	26.55	2,330,384
E1PG	0.54	7.19	7.21	21.37	33.65	33.75	2,324,291
E2PG	0.6	7.87	7.89	21.37	36.81	36.92	2,321,806
U2PG	1.39	6.12	6.28	21.36	28.65	29.38	2,330,623

Table 2 Mean value of daily RMS of the differences between the IGS GIMs and the JASON TEC by year (units: TECU)

Year	IGSG	C1PG	C2PG	E1PG	E2PG	U2PG
2009	2.52	3.42	3.43	3.63	3.86	3.03
2010	2.91	4.25	4.25	4.40	4.93	3.58
2011	3.94	5.18	5.30	6.00	6.57	5.65
2012	4.57	6.04	6.13	7.15	7.74	7.16
2013	4.57	5.80	5.83	7.06	7.75	6.09
2014	5.17	6.56	6.69	8.99	9.75	7.27
2015	4.73	6.11	6.31	8.19	8.94	7.12

their RMS and STD values are the lowest in most cases. All predicted IGS GIMs have a mean TEC value larger than or similar to the JASON data, which is compatible with the existence of the PEC. The averaged RMS results show that the performance of the 1-day predicted GIMs from a given IAAC (C1PG or E1PG) is better than the corresponding 2-day predicted GIMs (C2PG or E2PG). In addition, the CODE predicted GIMs (C1PG and C2PG) match the JASON TEC data better than the ESA and UPC predicted GIMs. In general, the results of the comparison against the JASON TEC data indicate that the order of performance of the predicted GIMs is C1PG, C2PG, U2PG, E1PG and E2PG.

In Table 2, the RMS values for the years 2009–2015 are shown for the differences between IGS final and predicted GIMs and JASON data. First, the changes in the RMS values obtained from the IGS final and predicted products over time are quite similar. The results show that the level of solar activity exerted a strong influence on the performance of the final and predicted GIM products. In particular, the RMS values increase gradually as the solar activity changes from low in 2009 to high in 2014. The 2-day UPC predicted product shows a better RMS performance compared to the CODE and ESA predicted products during low levels of solar activity (2009 and 2010), whereas the CODE predicted product yields slightly better results than the UPC and ESA predicted products during medium and high levels of solar activity (from 2011 to 2015).

To study the latitudinal behavior of the performance of predicted GIMs from different IAACs and the IGS combined

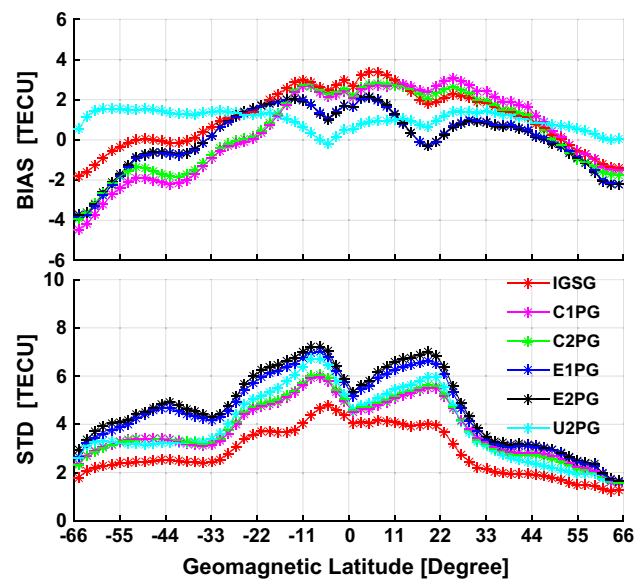


Fig. 3 Bias and STD values of the differences between the predicted and final GIM products and the JASON data. The assessed values were in two-degree geomagnetic latitude bins for the test period

final GIM product, the bias and STD of the differences between IGS GIMs and the external JASON data for multiple geomagnetic latitude bins (with bin widths of two degrees in this work) during the test period are shown in Fig. 3. A typical (inverted) U shape in terms of the geomagnetic latitude is seen in the figure, except for the 2-day UPC predicted

GIMs. The latitudinal dependence of the performance of IGS GIMs is in accordance with the findings of previous studies (García-Rigo et al. 2011). The positive discrepancies between the IGS GIMs and the JASON data in the equatorial and low-latitude regions represent the PEC between the orbital altitude of GPS satellites (20,200 km) and that of JASON satellites (1336 km). However, the IGS GIMs show lower TEC values than the JASON TEC in northern high-latitude and southern middle- to high-latitude regions. This pattern might be considered a fundamental limitation of the GNSS-based IGS GIMs and may be attributed to the scarcity of GNSS ground stations in data-poor regions, which are primarily oceans (Jee et al. 2010). Furthermore, the STDs of the differences for both final and predicted IGS GIMs with respect to the JASON data show a clear correlation with the effect of the Appleton-Hartree (equatorial) anomaly; STD values are found to be higher in the Southern Hemisphere than those in the Northern Hemisphere. Figure 3 also shows that the IGS combined final GIM product is always significantly better than all the predicted GIMs and that the 1- and 2-day ESA predicted GIMs feature larger STD values than the other IAAC predicted GIMs. Compared to the 2-day UPC predicted GIMs, the 1- and 2-day CODE predicted GIMs show slightly better performance at low latitudes and slightly worse performances at middle and high latitudes.

In order to identify whether predicted GIMs can provide correct predicted VTEC values during a geomagnetic event, taking the intense geomagnetic storm of March 17, 2015, as an example, we computed the RMS values of the differences between JASON observations and different IGS

GIMs. Obvious discrepancies among the TEC obtained from different sources are found, and the relative RMS of the TEC errors with respect to the JASON TEC data for IGSG, C1PG, C2PG, U2PG, E1PG and E2PG is 23, 70, 61, 68, 70 and 63%, respectively. Thus, the ability of all predicted IGS GIMs to model the ionospheric TEC during the geomagnetic event was not very good and needs to be further improved by accounting for the TEC disturbance induced by geomagnetic storms and other impulsive events to achieve better results during disturbed days. Note that the test results shown above during the geomagnetic event have been regarded as invalid and are not included in the statistics above.

Validation against GPS TEC

Figure 4 shows the time series of the bias and STD series for the final and predicted IGS GIMs compared to GPS TEC data. The bias and STD of each day are calculated based on the differences between the GIMs-interpolated TEC data and the GPS-derived TEC observations at all stations. The bias results show that the 2-day predicted UPC GIM has noticeable biases in the year 2012. Concerning the statistical results of the STD series in Fig. 4 and the RMS in Table 3, the IGS combined final GIM product has the best TEC value agreement with the GPS-derived VTEC data, and the CODE predicted GIMs have overall better accuracies than the other IAACs predicted GIMs.

In Table 4, the RMS values are shown by year for the differences between the GIMs and GPS data. Similar to the results of the comparison with JASON data, a strong

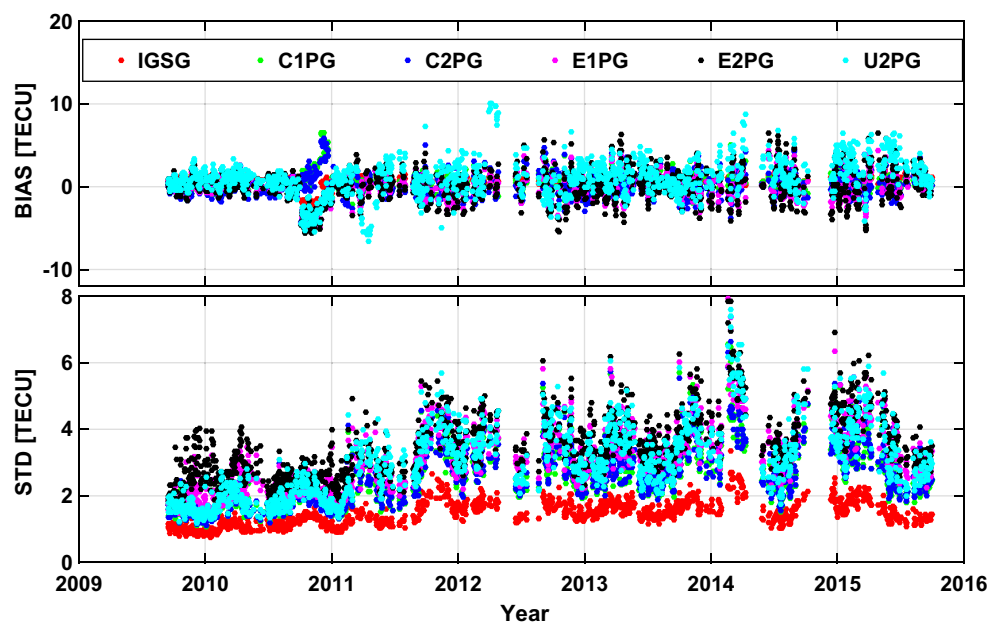


Fig. 4 Bias (top) and STD (bottom) of the differences between the predicted IGS GIMs and the ionospheric observations from GNSS stations for the test period

Table 3 Statistics of the RMS of ionospheric TEC obtained from IGS GIMs with respect to GPS TEC data for the test period (units: TECU)

	IGS	C1P	C2P	E1P	E2P	U2P
Mean	2.11	3.38	3.47	3.95	4.53	4.57
Maximum	4.26	9.03	8.41	8.95	9.78	11.65
Minimum	1.24	1.51	1.52	1.7	2.1	1.77

Table 4 Mean value of daily RMS of ionospheric TEC obtained from final and predicted IGS GIMs with respect to GPS TEC in each year (units: TECU)

Year	IGSG	C1PG	C2PG	E1PG	E2PG	U2PG
2009	1.70	2.09	2.13	2.58	3.26	2.59
2010	1.86	2.64	2.64	3.09	3.54	3.02
2011	2.12	3.24	3.38	3.68	4.21	4.54
2012	2.25	3.80	3.90	4.23	4.84	5.37
2013	2.24	3.76	3.87	4.32	4.91	4.79
2014	2.31	4.17	4.30	5.02	5.69	5.98
2015	2.21	3.77	3.92	4.65	5.34	5.86

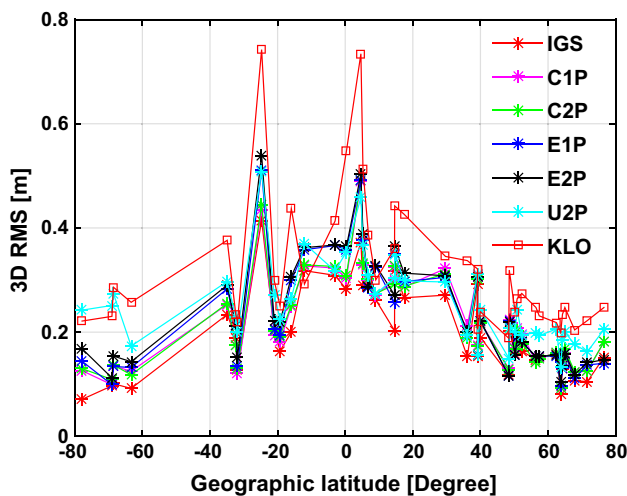


Fig. 5 3D RMS values of the differences between the estimated coordinates using different ionospheric corrections and the IGS-provided coordinates at the individual test stations for the test period. The stations are aligned by geographical latitudes on the horizontal axis

dependence on the level of solar activity is evident in the performance of the final and predicted GIM products.

In order to evaluate the performance of the predicted TEC in terms of SF PPP, we compare RMS statistics in the north, east, up and three-dimensional (3D) coordinate components based on the position solution errors within the last 4 h of the day. For comparison, the positioning results based on TEC corrections computed by the Klobuchar coefficients (named KLO) broadcasted in the navigation message are also presented. All the accessible stations listed in Fig. 2 were used in the verification. To compare the performance of the predicted GIMs at different latitudes, the averaged 3D RMS values for the test period are calculated for each individual station and plotted in Fig. 5. The averaged positioning

errors for different ionospheric correction cases at different latitudinal bands are also summarized in Fig. 6. The averaged RMS values for all selected stations for the test period are summarized in Table 5.

The positioning accuracies at stations located at mid- and high-latitude regions are much higher than those at stations located at low-latitude regions, as expected. The differences in the impacts of ionospheric corrections on positioning accuracy between different latitude bands are related to the latitudinal effect of the ionospheric activity level. Figures 5 and 6 show that the highest and lowest positioning accuracy can be obtained from the IGS combined final GIM product and the Klobuchar model, respectively. The results also show that the UPC 2-day predicted GIMs have slightly worse positioning performance compared to the other predicted GIMs. In summary, the comparison results in terms of SF PPP indicate that the order of performance of the predicted GIMs is C1PG, C2PG, E1PG, E2PG and U2PG.

Validation against the IGS combined final GIM products

The RMS, bias and STD series of the predicted GIMs from different IAACs with regard to the IGS combined final GIM product for the test period are shown in Figs. 7 and 8. The statistics of the differences, including the averaged bias, STD and RMS, are summarized in Table 6.

The CODE predicted GIM products systematically provide better results than the ESA and UPC products. The maximum RMS values among the different predicted IAACs GIMs occur on DOY 059 during the solar maximum peak, reaching values as high as 12.52 TECU in the U2PG GIMs, and the minimum RMS values occur on DOY 262 during the solar minimum peak, reaching values as low as 1.35 TECU in the C1PG GIMs. Similar to the results of the comparisons with

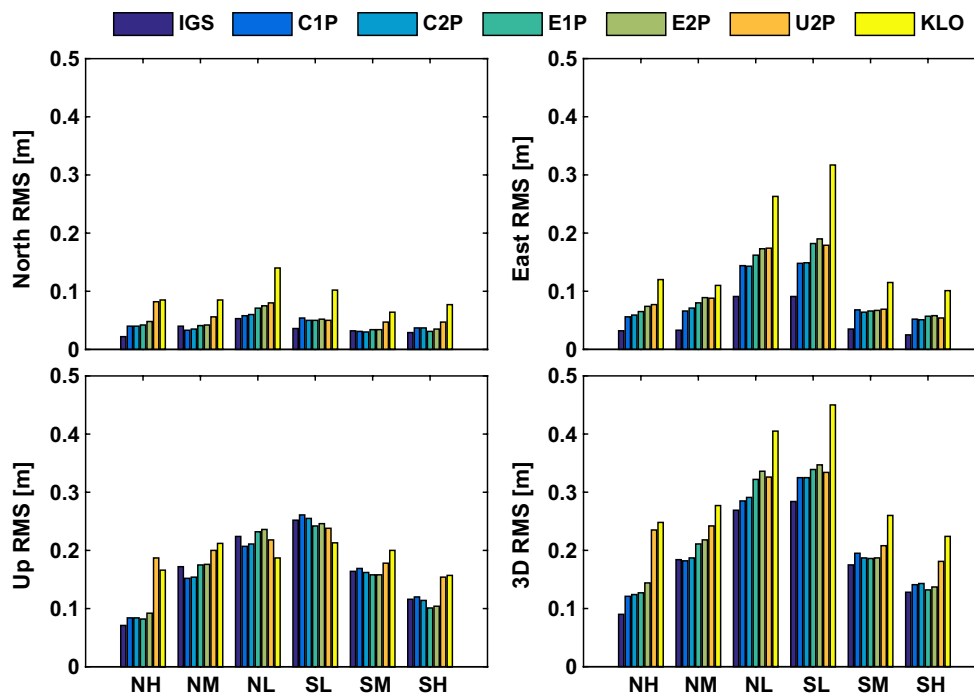


Fig. 6 Averaged positioning accuracy of SF PPP for selected stations located at different latitudes. The latitudinal bands for northern high latitudes, northern middle latitudes, northern low latitudes, southern

low latitudes, southern middle latitudes, and southern high latitudes are represented as NH, NM, NL, SL, SM, SH, respectively

Table 5 Averaged positioning accuracy at selected stations obtained with different ionospheric corrections for the test period (unit: dm)

	IGS	C1P	C2P	E1P	E2P	U2P	KLO
North	0.34	0.41	0.42	0.45	0.48	0.60	0.92
East	0.51	0.88	0.90	1.02	1.09	1.07	1.71
Up	1.60	1.61	1.63	1.67	1.70	1.96	2.06
3D	1.72	2.01	2.04	2.17	2.24	2.47	3.04

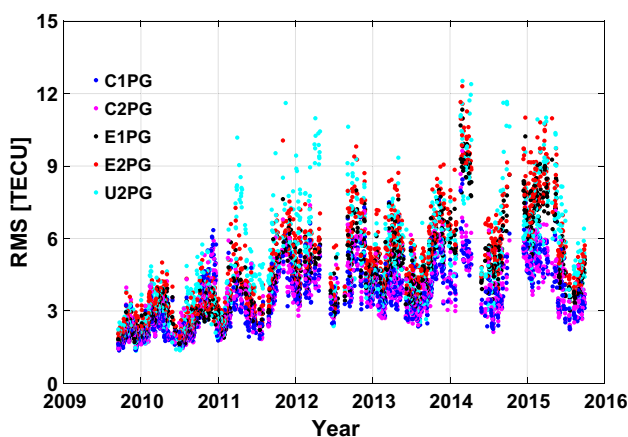


Fig. 7 RMS series of predicted GIMs from different IAACs with regard to the IGS combined GIM product for the test period

the JASON and GPS data, a strong dependence on the levels of solar activity is observed in the performance of the predicted GIM products in Table 7, which shows larger averaged RMS values for high levels of solar activity than for low levels of solar activity. Regarding the bias, note that although the averaged bias for U2PG against IGSG is only 0.02 TECU for the test period, larger fluctuations exist in the bias time series than in the other IAAC predicted GIMs. In general, the comparison results against the IGS combined final GIMs indicate that the order of performance of predicted GIMs is C1PG, C2PG, E1PG, U2PG and E2PG.

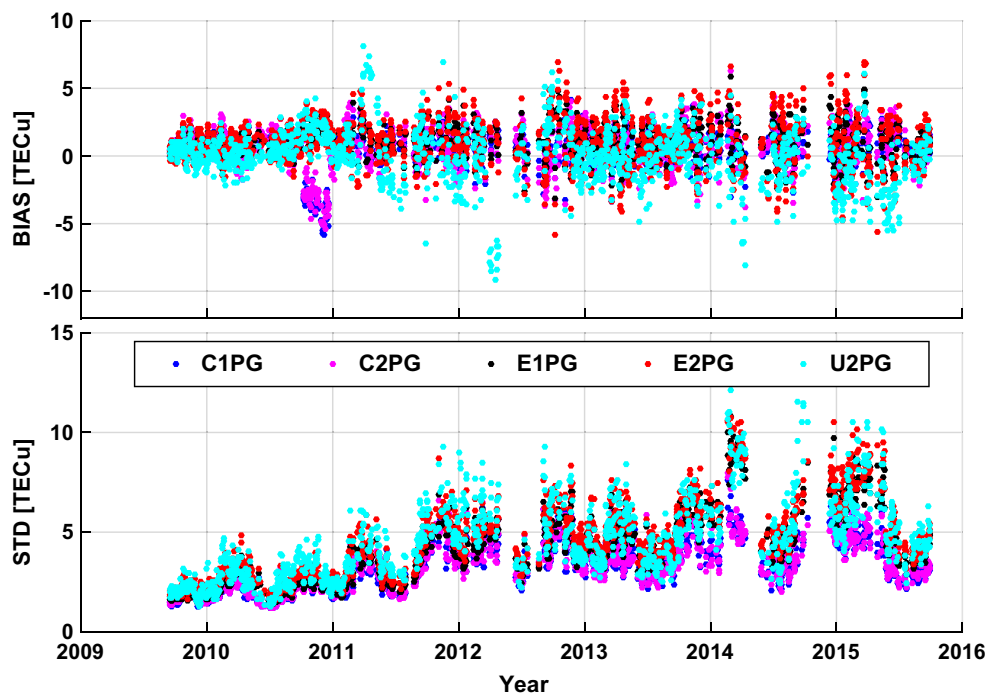


Fig. 8 Bias and STD series of predicted GIMs from different IGS IAACs with regard to the IGS combined GIM product for the test period

Table 6 Statistics of the differences between the predicted GIM VTEC data from the different IGS IAACs and the IGS combined final GIM product reference data, including bias, STD and RMS for the test period (units: TECU)

	C1PG	C2PG	E1PG	E2PG	U2PG
BIAS	0.51	0.52	0.98	0.98	-0.02
RMS	3.58	3.71	4.40	4.98	4.90
STD	3.27	3.31	4.06	4.53	4.44

Table 7 Mean value of daily RMS of differences between the predicted GIMs TEC from different IAACs and the IGS combined final GIM product reference data in each year (units: TECU)

	C1PG	C2PG	E1PG	E2PG	U2PG
2009	1.94	2.03	2.04	2.36	2.22
2010	2.72	2.75	2.71	3.08	3.06
2011	3.34	3.51	3.83	4.41	5.01
2012	4.27	4.41	4.89	5.64	5.98
2013	3.92	4.04	4.93	5.54	5.06
2014	4.39	4.57	6.49	7.18	6.70
2015	4.26	4.45	6.02	6.75	6.38

Conclusions

In this context, the accuracy of predicted GIMs produced by three different IAACs (CODE, UPC and ESA) has been evaluated. The goal was to provide information to SF GNSS users or related researchers to improve decision-making with respect to predicted GIM applications, such as real-time positioning. This experiment was performed through comparison with external TEC data sources provided by the JASON and GPS sources, as well as with the final combined GIM product, over both continental and oceanic regions from September 2009 to September 2015.

In general, although all of the predicted GIMs obtained from different IAACs can reliably reproduce the spatial and temporal variations in the TEC, there are significant discrepancies among these IAAC products. Mainly, the differences among the centers may depend on the different methods of computation and the differences among the mapping functions used in the TEC computation. This study shows that the CODE predicted GIMs exhibit better performance than the UPC and ESA predicted GIMs. The performance of the 1-day predicted GIMs from a given IAAC (C1PG or E1PG) is better than that of the corresponding 2-day predicted GIMs (C2PG or E2PG). The 2-day ESA and UPC predicted GIMs are found to have comparable performances. In addition, the UPC predicted GIMs show different performances for receiver-covered and ocean regions. Over ocean regions, compared to the 1- and 2-day CODE predicted GIMs, the

2-day UPC predicted GIMs show slightly worse performance at low latitudes and slightly better at middle and high latitudes. Over continental regions, the UPC predicted GIMs show slightly worse positioning performance than the other predicted GIMs. It is recommended that the CODE predicted GIMs be given first priority for the ionospheric prediction.

In accordance with the findings of previous studies, the dependence of latitude and of solar activities on the performance of predicted IGS GIMs has been determined in this study. Nevertheless, all of the predicted products show large relative errors above 60% with respect to JASON TEC data during a geomagnetic event; thus, these predictions need to be further improved by taking into account TEC disturbance information in order to achieve better performance on disturbed days.

Currently, the IAACs are attempting to improve the quality of their predicted TEC maps; thus, the results presented in this work are only based on the previous products. We believe that improvements to the predicted maps will have a positive impact on the final estimation of real-time ionospheric maps.

Acknowledgements Many thanks are due to the IGS for providing access to the ionospheric GIM products. This work was supported by the National Key Research Program of China “Collaborative Precision Positioning Project” (No. 2016YFB0501900), China Natural Science Funds (No. 41231064, 41674022, 41704038, 41574033 and 41621091), and the State Key Laboratory of Geodesy and Earth’s Dynamics (SKLGED2017-3-1-EZ).

References

- Azpilicueta F, Brunini C (2009) Analysis of the bias between TOPEX and GPS vTEC determinations. *J Geod* 83(2):121–127
- Brunini C, Azpilicueta FJ (2009) Accuracy assessment of the GPS-based slant total electron content. *J Geod* 83(8):773–785. <https://doi.org/10.1007/s00190-008-0296-8>
- Brunini C, Azpilicueta F (2010) GPS slant total electron content accuracy using the single layer model under different geomagnetic regions and ionospheric conditions. *J Geod* 84(5):293–304
- Brunini C, Meza A, Bosch W (2005) Temporal and spatial variability of the bias between TOPEX and GPS-derived total electron content. *J Geod* 79(4–5):175–188
- Cander LR (2003) Towards forecasting and mapping ionospheric space weather under COST actions. *Adv Space Res* 31(4):957–964
- Ciraolo L, Azpilicueta F, Brunini C, Meza A, Radicella S (2007) Calibration errors on experimental slant total electron content (TEC) determined with GPS. *J Geod* 81(2):111–120
- Feltens J (2003) The activities of the ionosphere working group of the international GPS service (IGS). *GPS Solut* 7(1):41–46. <https://doi.org/10.1007/s10291-003-0051-9>
- Feltens J, Angling M, Jackson-Booth N, Jakowski N, Hoque M, Hernández-Pajares M, Aragón-Ángel A, Orus R, Zandbergen R (2011) Comparative testing of four ionospheric models driven with GPS measurements. *Radio Sci* 46(6):RS0D12. <https://doi.org/10.1029/2010rs004584>
- García-Rigo A, Monte E, Hernández-Pajares M, Juan J, Sanz J, Aragón-Ángel A, Salazar D (2011) Global prediction of the vertical total electron content of the ionosphere based on GPS data. *Radio Sci* 46(6):RS0D25. <https://doi.org/10.1029/2010rs004643>
- Gulyaeva TL, Arikani F, Hernandez-Pajares M, Stanislawski I (2013) GIM-TEC adaptive ionospheric weather assessment and forecast system. *J Atmos Sol Terr Phys* 102:329–340. <https://doi.org/10.1016/j.jastp.2013.06.011>
- Hernández-Pajares M, Juan JM, Sanz J, Orus R, García-Rigo A, Feltens J, Komjathy A, Schaer SC, Krankowski A (2009) The IGS VTEC maps: a reliable source of ionospheric information since 1998. *J Geod* 83(3–4):263–275. <https://doi.org/10.1007/s00190-008-0266-1>
- Hernández-Pajares M, Roma-Dollase D, Krankowski A, García-Rigo A, Orus-Pérez R (2017) Methodology and consistency of slant and vertical assessments for ionospheric electron content models. *J Geod* 91(12):1405–1414. <https://doi.org/10.1007/s00190-017-1032-z>
- Hoque MM, Jakowski N, Berdermann J (2017) Ionospheric correction using NTCM driven by GPS Klobuchar coefficients for GNSS applications. *GPS Solut* 21(4):1563–1572. <https://doi.org/10.1007/s10291-017-0632-7>
- Jee G, Lee HB, Kim Y, Chung JK, Cho J (2010) Assessment of GPS global ionosphere maps (GIM) by comparison between CODE GIM and TOPEX/Jason TEC data: ionospheric perspective. *J Geophys Res Space Phys*. <https://doi.org/10.1029/2010JA015432>
- Keshin M (2012) A new algorithm for single receiver DCB estimation using IGS TEC maps. *GPS Solut* 16(3):283–292
- Komjathy A, Langley R (1996) An assessment of predicted and measured ionospheric total electron content using a regional GPS network. In: Proceedings of ION NTM 1996, Institute of Navigation, Santa Monica, CA, 22–24 January
- Komjathy A, Sparks L, Mannucci AJ, Coster A (2005) The ionospheric impact of the October 2003 storm event on Wide Area Augmentation System. *GPS Solut* 9(1):41–50. <https://doi.org/10.1007/s10291-004-0126-2>
- Krankowski A, Kosek W, Baran L, Popinski W (2005) Wavelet analysis and forecasting of VTEC obtained with GPS observations over European latitudes. *J Atmos Sol Terr Phys* 67(12):1147–1156
- Lambin J, Morrow R, Fu L-L, Willis JK, Bonekamp H, Lillibridge J, Perbos J, Zaouche G, Vaze P, Bannoura W (2010) The OSTM/Jason-2 mission. *Mar Geod* 33(S1):4–25
- Lee HB, Jee G, Kim YH, Shim JS (2013) Characteristics of global plasmaspheric TEC in comparison with the ionosphere simultaneously observed by Jason-1 satellite. *J Geophys Res Space Phys* 118(2):935–946
- Leick A, Rapoport L, Tatarnikov D (2015) GPS satellite surveying, 4th edn. Wiley, New York
- Li M, Yuan Y, Wang N, Li Z, Li Y, Huo X (2017) Estimation and analysis of Galileo differential code biases. *J Geod* 91(3):279–293
- Luo W, Liu Z, Li M (2013) A preliminary evaluation of the performance of multiple ionospheric models in low- and mid-latitude regions of China in 2010–2011. *GPS Solut* 18(2):297–308. <https://doi.org/10.1007/s10291-013-0330-z>
- Mannucci AJ, Wilson BD, Yuan DN, Ho CH, Lindqwister UJ, Runge TF (1998) A global mapping technique for GPS-derived ionospheric total electron content measurements. *Radio Sci* 33(3):565–582. <https://doi.org/10.1029/97rs02707>
- Orus R, Hernandez-Pajares M, Juan JM, Sanz J, Garcia-Fernandez M (2002) Performance of different TEC models to provide GPS ionospheric corrections. *J Atmos Sol Terr Phys* 64(18):2055–2062
- Orus R, Cander LR, Hernandez-Pajares M (2007) Testing regional vertical total electron content maps over Europe during the 17–21 January 2005 sudden space weather event. *Radio Sci* 42(3):RS3004. <https://doi.org/10.1029/2006rs003515>
- Schaer S (1999) Mapping and predicting the Earth’s ionosphere using the Global Positioning System. Doctoral dissertation, Univ. Bern, Switzerland

- Wang N, Yuan Y, Li Z, Huo X (2016) Improvement of Klobuchar model for GNSS single-frequency ionospheric delay corrections. *Adv Space Res* 57(7):1555–1569. <https://doi.org/10.1016/j.asr.2016.01.010>
- Wang N, Yuan Y, Li Z, Li Y, Huo X, Li M (2017) An examination of the Galileo NeQuick model: comparison with GPS and JASON TEC. *GPS Solut* 21(2):605–615
- Wielgosz P, Grejner-Brzezinska D, Kashani I (2003) Regional ionosphere mapping with kriging and multiquadric methods. *J Glob Position Syst* 2(1):48–55
- Yuan Y, Tscherning CC, Knudsen P, Xu G, Ou J (2008) The ionospheric eclipse factor method (IEFM) and its application to determining the ionospheric delay for GPS. *J Geod* 82(1):1–8. <https://doi.org/10.1007/s00190-007-0152-2>
- Yuan Y, Li Z, Wang N, Zhang B, Li H, Li M, Huo X, Ou J (2015) Monitoring the ionosphere based on the Crustal Movement Observation Network of China. *Geod Geodyn* 6(2):73–80. <https://doi.org/10.1016/j.geog.2015.01.004>
- Zolesi B, Cander LR (2014) *Ionospheric prediction and forecasting*. Springer, Berlin. <https://doi.org/10.1007/978-3-642-38430-1>



Min Li is a Ph.D. candidate at the Institute of Geodesy and Geophysics, Chinese Academy of Sciences. She received a B.S. degree from Shandong University of Science and Technology. Her current research interests include post and real-time GNSS ionospheric TEC modeling, determination of multi-GNSS differential code biases (DCBs), and space weather.



Yunbin Yuan is a professor and the director of GNSS Application and Research Group, Institute of Geodesy and Geophysics, Chinese Academy of Sciences. His current research interests are the following: (1) GNSS-based spatial environmental monitoring and analysis; (2) high-precision GNSS satellite navigation and positioning; (3) GNSS in orbit-determination applications for LEO satellites.



Ningbo Wang is a research assistant at the Academy of Opto-Electronics (AOE), Chinese Academy of Sciences (CAS), in Beijing, China. He received a Ph.D. degree in 2016 from the Institute of Geodesy and Geophysics, CAS. His work focuses on multi-GNSS differential code biases (DCBs) processing, global and regional real-time (RT) ionospheric TEC modeling based on multi-GNSS RT data.



Zishen Li is an associate researcher at the Academy of Opto-Electronics (AOE), Chinese Academy of Sciences (CAS), in Beijing, China. He received a Ph.D. degree in 2013 from the Institute of Geodesy and Geophysics, CAS. His current research activities are related to the ionospheric time delay corrections for precise GNSS/BDS applications.



Xingliang Huo is an associate professor at the Institute of Geodesy and Geophysics, Chinese Academy of Sciences. His current research interest is in the area of GNSS ionospheric tomography and the effects of ionospheric weather on GNSS navigation and positioning.